Carbohydrate Polymers 157 (2017) 1–8

Contents lists available at ScienceDirect

Carbohydrate Polymers

journal homepage: www.elsevier.com/locate/carbpol

Laponite as a rheology modifier of alginate solutions: Physical gelation and aging evolution

José Luis Dávila*, Marcos Akira d'Ávila

Department of Manufacturing and Materials Engineering, Faculty of Mechanical Engineering, University of Campinas, Campinas CEP 13083-860, Brazil

ARTICLE INFO

Article history:
Received 14 June 2016
Received in revised form
14 September 2016
Accepted 16 September 2016
Available online 17 September 2016

Keywords:
Laponite
Alginate
Rheology modifier
Polysaccharide
Gel point

ABSTRACT

The rheological behavior of alginate and Laponite/alginate solutions was studied. It was observed that the Cross viscosity model successfully describes the steady-state shear behavior of this polysaccharide. The scaling behavior analyzed for the entangled regime is in good agreement with polyelectrolyte solutions ($G_e \sim c_p^{3/2}$), with interactions generated between the alginate and the charged surfaces of the Laponite platelets. Therefore, the effect of Laponite as a rheology modifier is influenced by the alginate concentration. Higher alginate concentrations hindered the formation of the house of cards microstructure. Frequency sweep tests were performed to analyze the transition from solid-like to liquid-like behavior in a solid-like dominated domain. Soft physical gels were obtained at low alginate concentrations. The gel point was determined (1.65 wt.% of alginate and 2 wt.% of Laponite) through the Kramers–Krönig damping factor, and time sweep tests revealed the evolution of the storage (G') and loss modulus (G'') as functions of the waiting time (t_w). The growing elasticity revealed that Laponite/alginate solutions undergo aging.

1. Introduction

Alginate is an anionic polysaccharide that can be extracted from macroalgae or bacterial cultures. It is a copolymer of (1–4)-linked β-D-mannuronate (M) and α-L-guluronate (G) residues (Gacesa, 1988; Percival, 1979). The ratio of guluronic to mannuronic acid depends on the source. Alginates are block polymers; they are linear unbranched copolymers containing similar or strictly alternating blocks: MM, GG or GM. M and G acids are covalently linked, forming different sequences or blocks. Two adjacent G blocks can be cross-linked with multivalent cations: divalent cations such as Ca^{2+}, Ba^{2+}, Fe^{2+} or Sr^{2+} or trivalent cations such as Al^{3+}. Hence, a gelling mechanism occurs when those cations take part in ionic binding zones between G blocks (Augst, Kong, & Mooney, 2006; Rezende, Bártolo, Mendes, & Maciel Filho, 2009). Thereby, a three-dimensional network is formed. Binding zones are often called "egg boxes" (Larsen, Bjørnstad, Pettersen, Tønnesen, & Melvik, 2015; Papajová, Bujdoš, Chorvát, Stach, & Lacík, 2012; Percival, 1979; Venkatesan, Bhatnagar, Manivasagan, Kang, & Kim, 2015).

Alginate is a biopolymer characterized by its hydrophilicity. It can easily form aqueous solutions in which the viscosity increases with the alginate content and its molecular weight. Aqueous alginate solutions are non-Newtonian fluids, presenting shear-thinning behavior (Rezende et al., 2009). Due to its biocompatibility, non-toxicity and gelling mechanism, alginate has been widely used in tissue engineering applications, cell encapsulation, drug and protein delivery, and as pharmaceutical excipients, among other functions (Rodríguez-Rivero, Hilliou, del Valle, & Galán, 2014). Moreover, alginate is commonly used as a gelling agent in the food industry, textile/paper industry, and for dental impressions and wound dressings (Augst et al., 2006; Fu et al., 2011).

Laponite is a layered nanosilicate with the empirical formula $Na_{+0.7}[(Mg_{5.5}Li_{0.3})Si_8O_{20}(OH)_4]^{-0.7}$ (Perkins, Brace, & Matijević, 1974; Thompson & Butterworth, 1992; Xavier et al., 2015). It is a synthetic material obtained from a combination of salts of sodium, magnesium and lithium with sodium silicate. One of the applications of Laponite is as a rheology modifier (Ruzicka & Zaccarelli, 2011). It is an additive that promotes shear-thinning and thixotropic behavior in waterborne products (Willenbacher, 1996). In recent studies, Laponite was used to reinforce hydrogels for biomedical applications (Hong et al., 2015; Shen et al., 2014). Moreover, as reported by Xavier et al. (2015), nanocomposites reinforced with Laponite can support cellular adhesion and enhance in vitro mineralization and physiological stability, which expands the applications in the tissue engineering (TE) field. Laponite platelets are nanoscale disk-like particles with an aspect

* Corresponding author.
E-mail addresses: josedavila@fem.unicamp.br (J.L. Dávila), madavila@fem.unicamp.br (M.A. d'Ávila).

http://dx.doi.org/10.1016/j.carbpol.2016.09.057
0144-8617/

ratio of 1:25. They are formed in layers: two parallel sheets of tetrahedrally coordinated silica and a sheet of octahedrally coordinated magnesium oxide between them. Oxygen and OH^- groups are also present in the Laponite structure (Zulian, Ruzicka, & Ruocco, 2008). Furthermore, some magnesium atoms are substituted by lithium atoms. Therefore, a negative charge is on the platelet surfaces, whereas positive charges are on the rim due to the interlayer cations. In this case, the sodium ions balance the charges (Ruzicka & Zaccarelli, 2011). Conversely, when Laponite is dispersed in water, sodium ions are released, and the charges are unbalanced. Thus, the platelets adopt a negative charge on their faces, while the rims can adopt a positive or negative charge depending on the pH of the solution (Joshi, Reddy, Kulkarni, Kumar, & Chhabra, 2008; Kumar, Aswal, & Harikrishnan, 2016; Mongondry, Tassin, & Nicolai, 2005; Morariu, Bercea, & Sacarescu, 2014; Sun et al., 2012; Tawari, Koch, & Cohen, 2001).

Aqueous Laponite dispersions undergo physical aging because they are out of thermodynamic equilibrium. Hence, the microstructure of these dispersions progressively evolves to a lower level of energy (Jatav & Joshi, 2014; Shahin & Joshi, 2010). Thermal motion and particle aggregation due to the electrostatic forces between them influence physical aging (Jatav & Joshi, 2014; Labanda & Llorens, 2008), as do the Laponite concentration and the addition of polymers, salts or other components. It is reported in the literature that the intensity of the positive charges on the rims decreases as the pH increases; the rim is positively charged at pH ≤ 11 (Shahin & Joshi, 2010; Sun et al., 2012). With positive rims, a "house of cards" microstructure is formed by the platelets due to the electrostatic interactions between them and the faces (Liu & Bhatia, 2015; Mongondry et al., 2005). This microstructure is also responsible for the viscosity increase and the shear-thinning effect of aqueous Laponite dispersions (Mongondry et al., 2005). Under low shear rates, the house of cards structure is adopted, but it collapses at high shear rates. In this case, the platelets are oriented in the flow direction, and the viscosity decreases. Contrariwise, the negative charges on the rims have an influence on the elastic behavior of the dispersion due to the repulsion between platelets.

The electrostatic interaction between Laponite platelets and the mechanism of the formation of the microstructures are yet a matter of debate. The Laponite concentration plays an important role in the dispersion microstructure. Below a 2 wt.% Laponite concentration, the house of cards microstructure is suggested. Conversely, above this concentration, two proposals are suggested in the literature: (i) a house of cards or (ii) a Wigner repulsive glass microstructure. This latter takes into account the repulsion between Laponite platelets (Jatav & Joshi, 2014; Zulian et al., 2008). These microstructures evolve due to aging and can be destroyed by applying a deformation onto the sample, in a process called rejuvenation. The applied deformation should generate a stress greater than the yield stress of the sample (Jatav & Joshi, 2014). To perform rejuvenation, pre-shear or shear melting processes are carried out before the rheological studies. Sun et al. (2012) studied the aging phenomena in aqueous Laponite dispersions containing polyethylene glycol (PEG) and NaCl. To rejuvenate the samples to set a reference initial condition for the tests, a uniform shear field was applied. As observed in the dynamic time sweep test, a reproducible liquid state was achieved. Nevertheless, it is observed that the aging is partially irreversible, as described by Jatav and Joshi (2014); a shear melting process was previously applied to the rheological characterization of aqueous Laponite dispersions. In this case, an oscillatory shear stress was applied to rejuvenate the samples. As demonstrated, the shear melting rejuvenates the sample, although not completely; a slight difference is observed in comparison with a freshly prepared sample (Jatav & Joshi, 2014; Shahin & Joshi, 2010).

As previously described, the addition of salts and polymers modifies the aging of dispersions. Salt reduces the electrostatic repulsion between Laponite platelets, accelerating the aggregation for low concentrations of Laponite because the surface charge is screened (Sun, Wang, Wang, Liu, & Tong, 2013). The addition of salt also modifies the microstructure from glass-like to gel-like. The gel state has a fractal network, while the glass state does not have an ordered microstructure (Joshi et al., 2008).

The pronounced shear-thinning and solid-like behaviors provide interesting results for additive manufacturing (AM) applications in tissue engineering. Solutions rheologically modified could easily flow through nozzle tips due to the shear rate generated along their walls. Once out of a nozzle, the material could maintain its shape as result of the high viscosity (Barry et al., 2009; Hong et al., 2015). Subsequently, a crosslinking process can be applied to form hydrogels, thereby improving the geometric accuracy. In this work, the rheological behavior of alginate aqueous solutions and Laponite/alginate solutions was studied. A steady-state shear master curve for alginate solutions was obtained. When Laponite was added to the alginate solutions, a pronounced shear-thinning behavior was observed in steady-state shear tests. Then, frequency sweep tests were performed to analyze the physical gelation due to the electrostatic interactions between the Laponite platelets and alginate chains. The damping factor of the solutions was analyzed as a function of the alginate concentration, where the gelation mechanism, which arises due to the dispersed Laponite platelets, was studied. Finally, time sweep tests were performed to analyze the aging evolution of the Laponite/alginate samples under the gel point concentration.

2. Experimental

2.1. Materials and solution preparation

Medium-viscosity sodium alginate from brown algae was purchased from Sigma–Aldrich Corp., USA. Its molecular weight ranges between 80,000 and 120,000 g mol^{-1}, and it is composed of approximately 61% mannuronic acid and 39% guluronic acid. Laponite XLG was obtained from Southern Clay Products, Inc., USA. Sodium chloride was purchased from Labsynth, Brazil. 0.1 M NaCl was added to the dilute alginate solutions to determine the viscosity-average molecular weight using the Mark–Houwink–Sakurada correlation, which is given by

$$[\eta] = KM^{\alpha} \tag{1}$$

where $[\eta]$ is the intrinsic viscosity, $K = 7.3 \times 10^{-3}$ g ml^{-1} and $\alpha = 0.92$ for an M/G ratio of 1.56 (Thu et al., 1996). The specific and reduced viscosities are given by Eqs. (2) and (3), respectively,

$$\eta_{sp} = \frac{\eta_0 - \eta_s}{\eta_s} \tag{2}$$

$$\eta_{red} = \frac{\eta_{sp}}{c_p} \tag{3}$$

where η_0 is the zero shear viscosity, η_s the solvent viscosity (η_s = 0.001003 Pa s at 20 °C) and c_p the polymer concentration. The intrinsic viscosity is given by

$$[\eta] = \lim_{c_p \to 0} \left(\frac{\eta_{sp}}{c_p} \right) \tag{4}$$

All solutions were prepared using deionized water without added NaCl, except that to determine the viscosity-average molecular weight. Alginate solutions and Laponite/alginate solutions were prepared using a magnetic stirrer for 6 h with a plate temperature of 60 °C to ensure homogeneity. All samples were stored for 16 h before the rheological tests. The Laponite/alginate solutions were prepared using 2 wt.% Laponite. The alginate concentration was varied in the range of 0.25–4 wt.% for the steady-state shear and

frequency sweep tests. For the time sweep tests, alginate concentrations with a solid-like behavior (0.25–1 wt.%) were analyzed. To prepare the solutions, it was necessary to completely disperse and hydrate the Laponite before the addition of the alginate. Laponite was dispersed in deionized water using a vortex agitator. It was added gradually into the water over a period of 10–30 s to reduce the dispersion time, and a clear colorless solution was obtained in approximately 20 min. The pH of the solutions was measured using samples of approximately 10 ml in a Tecnal TEC-5 pH meter.

2.2. Rheological characterization

The rheological characterization of the solutions was performed using an Anton Paar MCR-102 Modular Compact Rheometer. Tests were conducted using a cone-plate geometry (CP50-1) with a 50 mm diameter, a cone angle of 0.9815° and a truncation of 0.97 μm. To determine the viscosity-average molecular weight, steady-state shear tests were performed at 20 °C (Fig. S1 of the supplementary material), while all the other experiments were performed at 25 °C. The rheological characterizations were carried out using a solvent trap to prevent water evaporation. Before each test, a constant pre-shear of 200 s^{-1} was applied for 300 s to avoid any memory effect and rejuvenate the samples (pre-shear curves are illustrated in Fig. S2 of the supplementary material). Measurements of the shear rate in the steady state were performed in the range of 0.001–700 s^{-1}. Amplitude sweep tests were carried out at an angular frequency of 10 rad s^{-1} to obtain the linear viscoelasticity (LVE) range (γ_0 = 1% for all samples). Next, frequency sweep tests were conducted in the range of 0.1–200 rad s^{-1}. Finally, time sweep tests were performed to study the aging evolution. Each time sweep test was carried out for 1000 s, and the angular frequency was varied from 10 to 100 rad s^{-1}.

3. Results and discussion

3.1. Steady-state shear characterization

Initially, the intrinsic viscosity was obtained by a linear fit of the curve of reduced viscosity versus alginate concentration (Fig. S1 of the supplementary material). Then, using the Mark–Houwink–Sakurada correlation, a viscosity-average molecular weight of 99,986 g mol^{-1} was calculated, which is inside the range of molecular weights provided by the supplier (80,000–120,000 g mol^{-1}). Next, different concentrations of alginate solutions were studied. As observed in Fig. 1a, when the alginate concentration increases, the viscosity of the solution also increases. Shear-thinning behavior can be observed for all cases, even in low-concentration solutions. In the range of shear rates

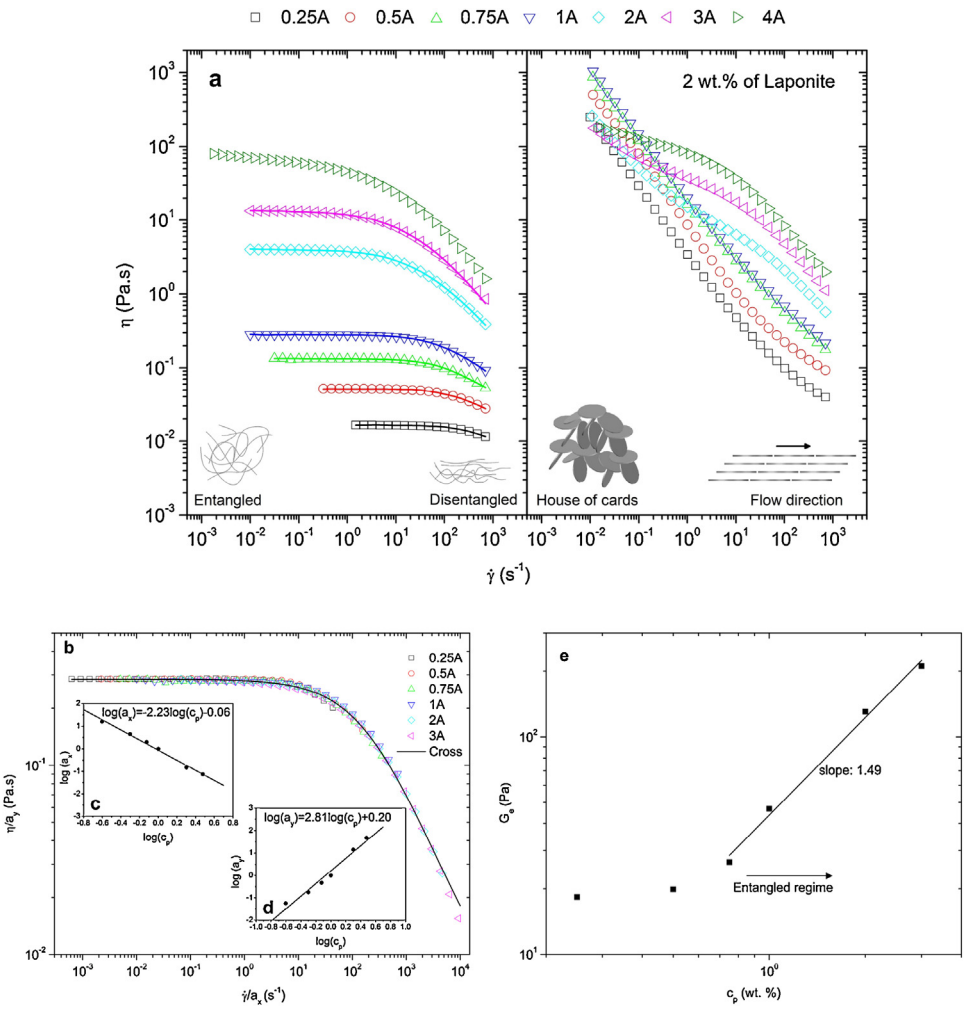

Fig. 1. (a) Viscosity curves for aqueous alginate and Laponite/alginate solutions. Open symbols correspond to experimental data. Solid lines correspond to the Cross model fitting for alginate. Inset schemes describe the mechanisms that contribute to the shear-thinning behavior, (b) alginate viscosity master curve (reference concentration 1 wt.%), (c) and (d) horizontal (a_x) and vertical (a_y) shift factors vs. concentration and (e) plateau modulus as a function of the alginate concentration (results were scaled for the entangled regime).

Table 1
Shift factors for experimental viscosity master curve and fitting parameters for Cross model.

Experimental						
c_p (wt.%)	0.25	0.5	0.75	1	2	3
a_x	16	4.5	2	1	0.15	0.075
a_y	0.0574	0.178	0.473	1	14.072	47.607
Fit						
c_p (wt.%)	η_∞ (Pa s)	η_0 (Pa s)	$\dot{\gamma}_c$ (s^{-1})	n	*MRD* (%)	
0.25	0.0039	0.0165	1111.1	0.9999	0.4	
0.5	0.0143	0.0517	384.6	0.9999	0.6	
0.75	0.0319	0.1327	200.0	0.9998	0.8	
1	0.0413	0.2806	166.7	0.9164	0.5	
2	0.0169	3.9892	32.7	0.7415	0.5	
3	0	13.5352	15.6	0.7094	1.5	
Master curve	0.0036	0.2847	204.08	0.7484	1.9	

studied, all compositions, except for the one with 4 wt.% of alginate, exhibit a Newtonian plateau. The shear-thinning is associated with an entangled network and is the typical behavior of polymer solutions (Yu, Zhang, Luan, Zhang, & Zhang, 2014). Next, using the steady-state shear viscosity data obtained, a master curve was constructed. This method has been applied successfully in other polysaccharide solutions (Gorret, Renard, Famelart, Maubois, & Doublier, 2003; Payet, Ponton, Grossiord, & Agnely, 2010). The vertical and horizontal shift factors were calculated using as references a 1 wt.% alginate concentration, the zero shear viscosity for the vertical axis and the initial point of shear-thinning behavior for the horizontal axis. As observed in Fig. 1b, the viscosity master curve shows that the superimposed data have a common mechanism that governs the alginate viscoelasticity. The shear-thinning behavior is generated due to the disentanglement of the polymer chains. These chains need time to relax, and then the transition from the Newtonian plateau to shear-thinning behavior occurs at a critical shear rate equal to the inverse of the relaxation time. In addition, Fig. 1b shows the fitted master curve using the Cross model, which successfully describes the shear-thinning behavior of polysaccharide solutions (Roger et al., 2015). This model is given by

$$\eta(\dot{\gamma}) = \eta_\infty + \frac{\eta_0 - \eta_\infty}{1 + \left(\dot{\gamma}/\dot{\gamma}_c\right)^n} \tag{5}$$

where η_∞ is the infinite shear viscosity, η_0 the zero shear viscosity, $\dot{\gamma}$ the shear rate, $\dot{\gamma}_c$ the critical shear rate, and n the power-law index. As observed in Fig. 1b–d, the Cross model fits the experimental results quite well, especially for the lower shear rates. The Carreau model also describes the shear-thinning behavior, but as reported by Payet et al. (2010), the Cross model fits better, especially at high shear rates. Table 1 summarizes the experimental and fitting parameters and the mean relative deviations (MRD) of the fitted curves.

The scaling behavior of the plateau modulus, which describes the chain entanglement effects (Yu et al., 2014) in the alginate solutions, was determined by rheological data. This modulus can be calculated by

$$G_e = \frac{\eta_0}{\lambda} \tag{6}$$

where λ is the relaxation time, calculated as the inverse of the shear rate at which the transition from Newtonian to shear-thinning behavior occurs. In Fig. 1e are shown the scaled results for entangled solutions. As observed, they are consistent with the scaling law for polyelectrolyte solutions ($G_e \sim c_p^{3/2}$) (Colby, 2010; Yu et al., 2014). Nevertheless, a recent study reported that the exponential value of the scaling behavior could be higher than (3/2); an exponent between 2 and 3 is suggested due to the monomers' dipolar interactions through counterions (Roger et al., 2015). For high polymer concentrations, the electrostatic interactions of the polyelectrolytes can be neglected, and the behavior could be similar to that of a good solvent scaling exponent (2.25) (Dou & Colby, 2006). Charged surfaces cause the adsorption of polyelectrolytes. Therefore, the anionic polyelectrolyte behavior of the alginate solutions generates interactions with the charged Laponite particles. As observed in Fig. 1a, the viscosity curves of Laponite/alginate solutions show the influence of Laponite on the rheological behavior. In all cases, the viscosity decreases when the shear rate increases. At low shear rates, a high viscosity is observed in comparison to that of the alginate solutions. Conversely, a low viscosity is observed for high shear rates. In Laponite/alginate solutions, the shear-thinning effect would be associated with the disentanglement of polymer chains and the Laponite platelet orientation in the flow direction (Aalaie, 2012). As a result, at high shear rates, these solutions exhibit little resistance to flow. When the shear rate is reduced, the alginate chains become entangled. Moreover, the Laponite platelets form a house of cards structure, considerably increasing the viscosity in comparison to that of alginate solutions. This structure is formed due to electrostatic interactions (Mongondry et al., 2005). At low

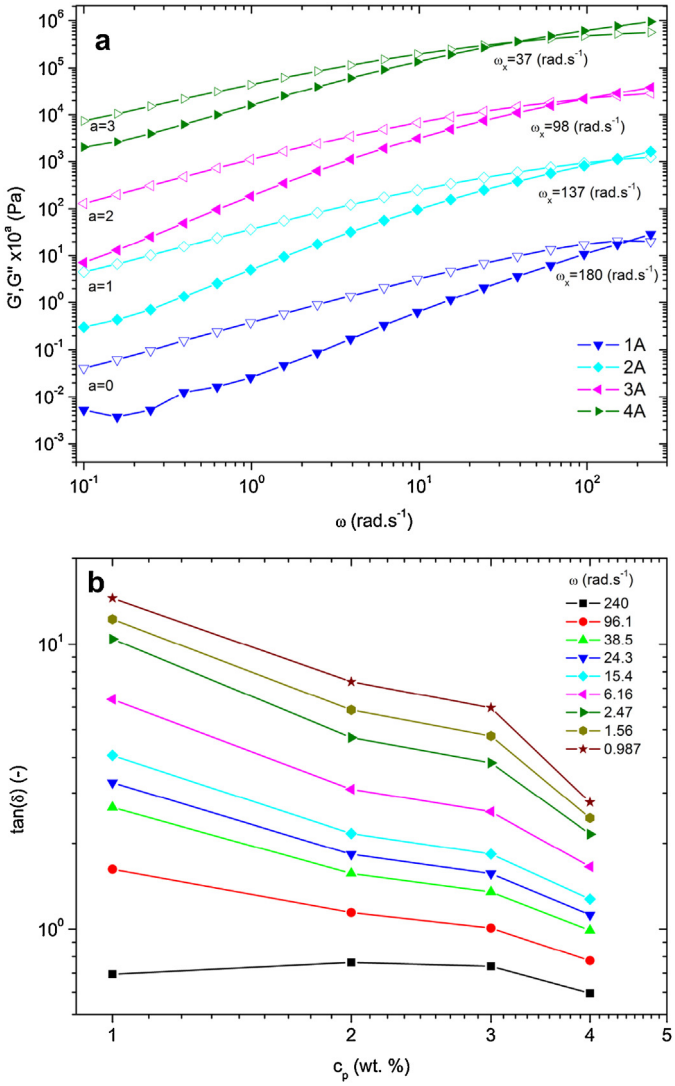

Fig. 2. (a) Dependence of G' (solid symbols) and G'' (open symbols) on the angular frequency for alginate solutions in entangled regime (data are vertically shifted to avoid overlapping) and (b) damping factor plotted against the alginate concentration for different angular frequencies.

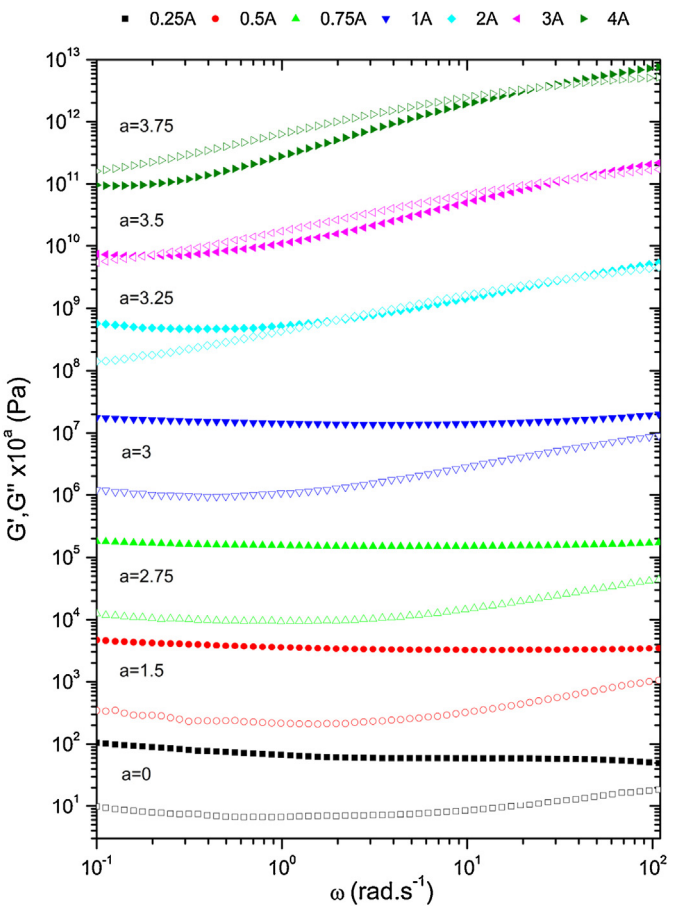

Fig. 3. Dependence of G' (solid symbols) and G'' (open symbols) on the angular frequency for 2 wt.% Laponite in the presence of different alginate compositions (data are vertically shifted to avoid overlapping).

shear rates, a gel structure forms if Laponite is properly incorporated into the solution. Contrariwise, at high shear rates, the house of cards structure completely disappears due to shear forces. Hence, a pronounced shear-thinning behavior is observed. Additionally, as observed in Fig. 1a, higher alginate concentrations hinder the effect of Laponite as a rheology modifier due to polymer adsorption on the Laponite surfaces. This is associated with the polyelectrolyte behavior previously described. Therefore, in Laponite/alginate solutions, for high alginate concentrations, the viscosity curves differ slightly from those of alginate solutions.

3.2. Physical gelation

To analyze the physical gelation generated due to the interactions between Laponite and alginate, frequency sweep tests were performed. Fig. 2a shows the results for alginate solutions in the entangled regime. For all cases, a crossover point defines the transition from a liquid-like dominated domain ($G'' > G'$) to a solid-like dominated domain ($G' > G''$). As shown, the crossover frequency (ω_x) is higher for lower alginate concentrations. This frequency is often associated with the longest relaxation time of the material, which is calculated as the inverse of the crossover frequency. Hence, the relaxation time increases as a function of the alginate concentration. This time defines the period in which the polymer chains can disentangle as a result of the oscillating shear applied. Longer chains cannot disentangle, which causes the transition from liquid-like to solid-like behavior (Yu et al., 2014). Fig. 2b shows the damping factor ($\tan(\delta) = G''/G'$) as a function of the alginate concentration. As shown, at high frequencies, the solid-like behavior

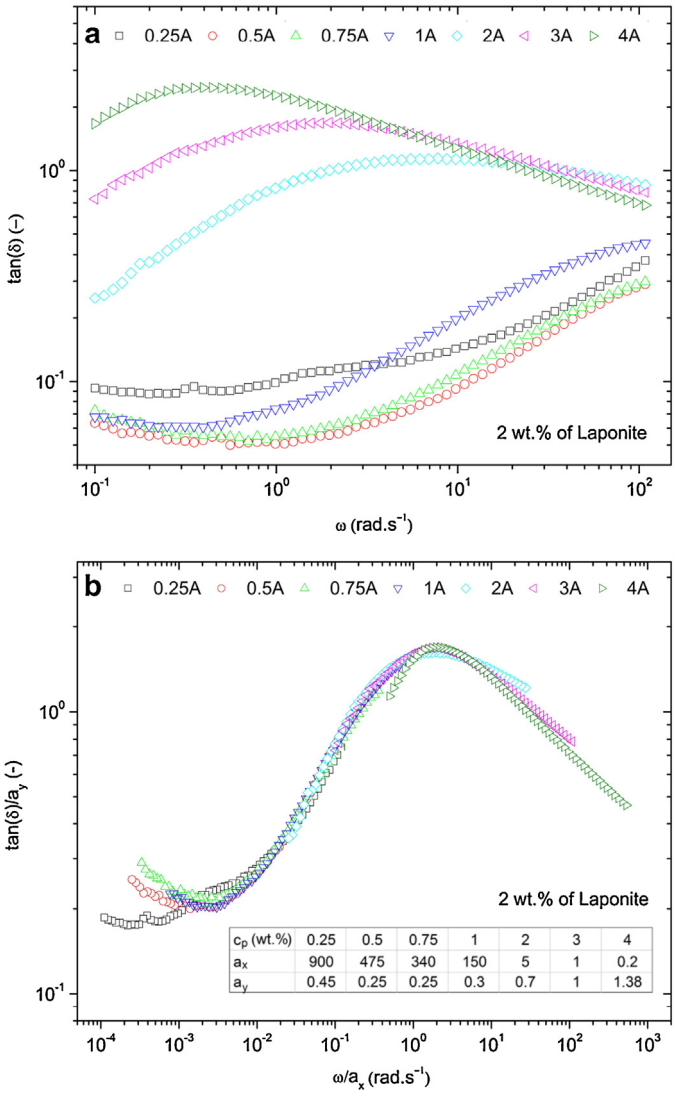

Fig. 4. (a) Damping factor plotted against angular frequency and (b) damping factor superimposed curve for Laponite/alginate solutions (inset table shows the horizontal (a_x) and vertical (a_y) shift factors. Reference concentration: 3 wt.% alginate).

Table 2
pH values for Laponite/alginate solutions.

c_L (wt.%)	0.25 A	0.5 A	0.75 A	1 A	2 A	3 A	4 A
0	6.86	6.85	6.87	7.51	7.34	7.52	7.94
2	9.99	9.82	9.63	9.74	9.51	9.18	9.12

is dominating ($\tan(\delta) < 1$). Moreover, the damping factor decreases when the alginate concentration increases. This is, larger amounts of polymer contribute to the solid-like behavior, thus decreasing $\tan(\delta)$.

On the other hand, Fig. 3 shows the storage and loss moduli as functions of the angular frequency for Laponite/alginate solutions. As shown, soft gels were obtained at low alginate concentrations. Taking into account that aqueous alginate solutions are polyelectrolytes, alginate could adsorb on an oppositely charged surface, in this case, the charged surfaces of Laponite. Table 2 shows the pH values for alginate and Laponite/alginate solutions; as observed, pH < 11 for all cases. Hence, it is suggested that alginate, which is an anionic polymer, is being adsorbed on the positively charged surface of the Laponite, in this case, the rim of the platelets. As a result, when the alginate concentration increases, a

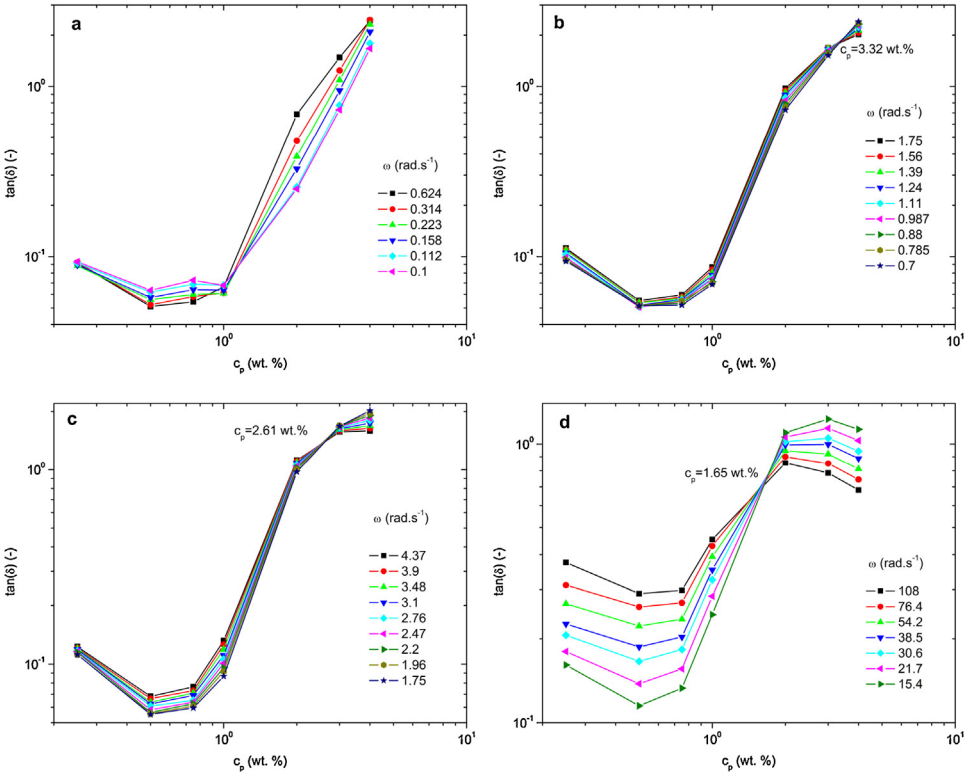

Fig. 5. Damping factor plotted against the alginate concentration. Frequency increases from (a) to (d).

transition from solid-like to liquid-like behavior is observed. At low alginate concentrations, physical gelation occurs as a result of Laponite–alginate interactions. Conversely, alginate adsorption on Laponite surfaces at higher alginate concentrations hinders the rheology modifier effect because the formation of the house of cards structure is difficult. Fig. 4a shows the damping factor plotted against the angular frequency. This curves were superimposed by horizontal and vertical shifting, as illustrated in Fig. 4b, revealing that the transition from a dominant solid-like behavior to a liquid-like behavior follows a similar route when the alginate concentration increases and the Laponite concentration is maintained fixed at 2 wt.%.

The transition from solid-like to liquid-like behavior can be analyzed through the damping factor. This transition is defined by the gel point. The damping factor from Kramers-Krönig is defined by Eq. (7) (Liu, Qian, Shu, & Tong, 2003), which has no dependence on the angular frequency at the gel point:

$$\tan\left(\delta\right) = \frac{G''}{G'} = \tan\left(\frac{n\pi}{2}\right) \tag{7}$$

The gel point is defined by the relaxation modulus $G(t)$ of a critical gel. This modulus was proposed by Winter and Chambon (1986), as a power-law described by

$$G(t) = St^{-n} \tag{8}$$

where S is the gel strength and n the relaxation exponent ($0 < n < 1$). The gel strength can be determined by Eq. (9) at the gel point (Jatav & Joshi, 2014),

$$G' = \frac{G''}{\tan\left(\frac{n\pi}{2}\right)} = S\omega^n \Gamma(1-n)\cos\left(\frac{n\pi}{2}\right) \tag{9}$$

where $\Gamma()$ is the gamma function. Therefore, the gel strength can be calculated by obtaining n from Eq. (8) and G' or G''.

Fig. 5 shows plots of the damping factor against the alginate concentration for different frequencies. Fig. 5a reveals that the solid-like behavior dominates at small frequencies for alginate concentrations under 1 wt.%, while, Fig. 5b and c show no frequency dependence at $c_p = 2.61$ wt.% and $c_p = 3.32$ wt.%. At these concentrations, transitions from solid-like to liquid-like behavior occur in a liquid-like dominated domain ($\tan(\delta) > 1$). Moreover, Fig. 5d shows no frequency dependence at $c_p = 1.65$ wt.% and $\tan(\delta) = 0.73$. At this concentration, a transition from solid-like to liquid-like behavior occurs in a solid-like dominated domain ($\tan(\delta) < 1$). Therefore, at this concentration, the gel point is defined, below which, soft gels were obtained. When the alginate concentration increases, a progressive increase in the damping factor is observed, suggesting a reduction in the elasticity. This fact explains the considerable reduction of the shear-thinning effect of Laponite when the alginate concentration increases. Furthermore, as observed in Fig. 5, the plotted data are mainly in the region $\tan(\delta) < 1$. That is, the solid character of the material prevails over the viscous ($G' > G''$). In contrast, the damping factor of alginate solutions previously shown in Fig. 2b shows that plotted data are mainly in the region $\tan(\delta) > 1$. Moreover, when the alginate concentration increases, the elasticity also increases for the alginate solutions and decreases in the Laponite/alginate solutions. For this reason, soft gels are formed mainly at lower alginate concentrations.

3.3. Aging evolution

Fig. 6a shows the storage modulus (G') and the loss modulus (G'') obtained through time sweep tests carried out at different angular frequencies for the composition of 0.25 wt.% alginate and 2 wt.% Laponite. As observed, G' increases as a function of the waiting time (t_w) and the angular frequency (ω). Similar behavior was observed for the other compositions (for clarity, only one composition was depicted, while the other compositions are illustrated in Fig. S3 of the supplementary material). G'' also increases with the frequency, but slightly decreases at low waiting times and remains constant at high waiting times. G' is higher than G'', corroborating a solid-like

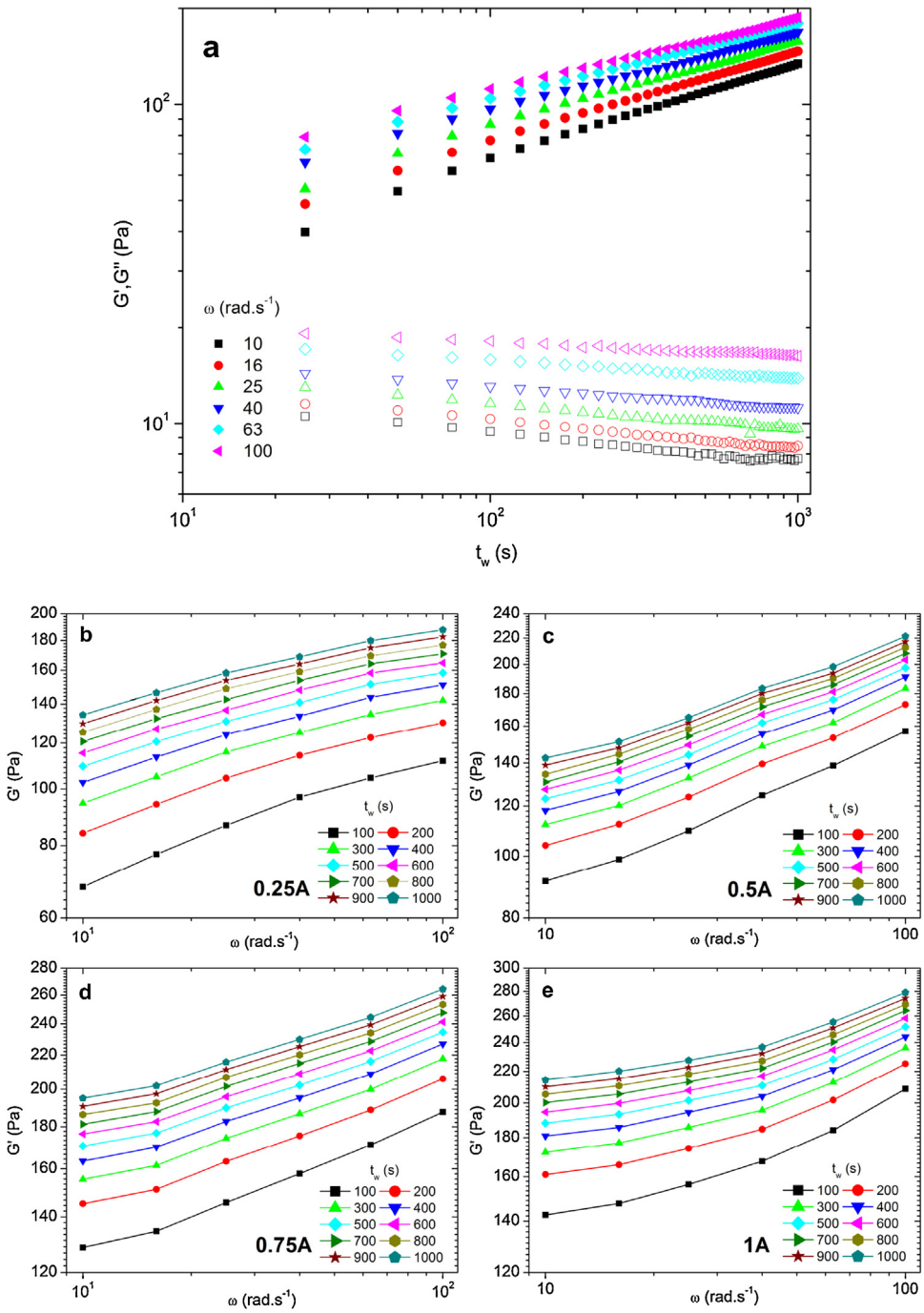

Fig. 6. Aging evolution: (a) dependence of G' (solid symbols) and G'' (open symbols) on the waiting time (t_w) for frequencies in the range of 10–100 rad s^{-1} for the composition 0.25 wt.% alginate and 2 wt.% Laponite and (b–e) reconstructed frequency dependence of G' for different waiting times (t_w).

behavior when the aging was analyzed in compositions under the gelling point. Hence, the damping factor decreases with the waiting time, which demonstrates a growing Hookean elasticity (Sun et al., 2012). Moreover, the frequency dependence of G' was reconstructed, which is depicted in Fig. 6b–e for different compositions and waiting times. In these curves, there can be clearly observed a growing elasticity as a function of the waiting time and frequency. The storage modulus also increases with the alginate concentration due to the structural interactions generated between the polymer chains and the Laponite platelets over time. Then, the evolution of the elastic behavior demonstrates that Laponite/alginate solutions undergo aging.

4. Conclusions

Rheological studies performed in alginate and Laponite/alginate solutions allowed the analysis of the mechanism that influences the transition from a shear-thinning behavior in alginate solutions to a pronounced shear-thinning behavior when Laponite is added. Electrostatic interactions between charged Laponite platelets generate a house of cards structure when the shear rate tends to zero. Therefore, at low shear rates, the entangled alginate chains and the house of cards structure contribute to increasing the viscosity considerably. In addition, a solid-like dominated behavior arises due to interactions between the alginate chains and Laponite platelets. As

demonstrated, alginate solutions have a polyelectrolyte behavior ($G_e \sim c_p^{3/2}$). Therefore, taking into account that alginate is an anionic polysaccharide and the rim of the Laponite platelets is positively charged at pH ≤ 11, it is suggested that the alginate adsorbs on the positive surfaces of Laponite, which hinders the increase in viscosity at high alginate concentrations. Frequency sweep tests revealed that Laponite produces physical gelation in alginate solutions. Moreover, the damping factor from Kramers–Krönig allowed the determination of the gel point. This last factor defines the transition from solid-like to liquid-like behavior, which follows a similar route, as revealed by a superimposed curve. As observed, at the gel point, the damping factor has no dependence on the frequency. Finally, time sweep tests revealed a growing elasticity as a function of the waiting time. Hence, Laponite/alginate solutions undergo aging. Furthermore, it is anticipated that Laponite/alginate solutions together with AM processes have potential applications in tissue engineering. To crosslink the solutions to form hydrogels, the rheological characterizations of the chemical gelation will be included in future studies.

Acknowledgements

The authors acknowledge the Secretaría de Educación Superior, Ciencia, Tecnología e Innovación (SENESCYT-Ecuador) and the Conselho Nacional de Desenvolvimento Científico e Tecnológico (CNPq-Brazil), Proj. N°401297/2014-4 and Proj. N°308660/2015-3. J.L. Dávila expresses thanks for the Ph.D. fellowship N°AR2Q-8590 from SENESCYT.

Appendix A. Supplementary data

Supplementary data associated with this article can be found, in the online version, at http://dx.doi.org/10.1016/j.carbpol.2016.09.057.

References

Aalaie, J. (2012). Rheological behavior of polyacrylamide/laponite nanoparticle suspensions in electrolyte media. *Journal of Macromolecular Science, Part B*, *51*, 1139–1147.

Augst, A. D., Kong, H. J., & Mooney, D. J. (2006). Alginate hydrogels as biomaterials. *Macromolecular Bioscience*, *6*, 623–633.

Barry, R. A., Shepherd, R. F., Hanson, J. N., Nuzzo, R. G., Wiltzius, P., & Lewis, J. A. (2009). Direct-write assembly of 3d hydrogel scaffolds for guided cell growth. *Advanced Materials*, *21*, 2407–2410.

Colby, R. H. (2010). Structure and linear viscoelasticity of flexible polymer solutions: Comparison of polyelectrolyte and neutral polymer solutions. *Rheologica Acta*, *49*, 425–442.

Dou, S., & Colby, R. H. (2006). Charge density effects in salt-free polyelectrolyte solution rheology. *Journal of Polymer Science Part B: Polymer Physics*, *44*, 2001–2013.

Fu, S., Thacker, A., Sperger, D. M., Boni, R. L., Buckner, I. S., Velankar, S., Munson, E. J., & Block, L. H. (2011). Relevance of rheological properties of sodium alginate in solution to calcium alginate gel properties. *Aaps Pharmscitech*, *12*, 453–460.

Gacesa, P. (1988). Alginates. *Carbohydrate Polymers*, *8*, 161–182.

Gorret, N., Renard, C., Famelart, M., Maubois, J., & Doublier, J. (2003). Rheological characterization of the EPS produced by P. acidi-propionici on milk microfiltrate. *Carbohydrate Polymers*, *51*, 149–158.

Hong, S., Sycks, D., Chan, H. F., Lin, S., Lopez, G. P., Guilak, F., Leong, K. W., & Zhao, X. (2015). 3d printing of highly stretchable and tough hydrogels into complex, cellularized structures. *Advanced Materials*, *27*, 4035–4040.

Jatav, S., & Joshi, Y. M. (2014). Rheological signatures of gelation and effect of shear melting on aging colloidal suspension. *Journal of Rheology (1978-present)*, *58*, 1535–1554.

Joshi, Y. M., Reddy, G. R. K., Kulkarni, A. L., Kumar, N., & Chhabra, R. P. (2008). Rheological behaviour of aqueous suspensions of laponite: New insights into the ageing phenomena. *Proceedings of the Royal Society of London A: Mathematical, physical and engineering sciences* (Vol. 464) (pp. 469–489). The Royal Society.

Kumar, S., Aswal, V. K., & Harikrishnan, G. (2016). Polymer concentration regulated aging in aqueous laponite suspensions. *Rheologica Acta*, *55*, 411–421.

Labanda, J., & Llorens, J. (2008). Effect of aging time on the rheology of laponite dispersions. *Colloids and Surfaces A: Physicochemical and Engineering Aspects*, *329*, 1–6.

Larsen, B. E., Bjørnstad, J., Pettersen, E. O., Tønnesen, H. H., & Melvik, J. E. (2015). Rheological characterization of an injectable alginate gel system. *BMC Biotechnology*, *15*, 1.

Liu, X., & Bhatia, S. R. (2015). Laponite® and laponite® -PEO hydrogels with enhanced elasticity in phosphate-buffered saline. *Polymers for Advanced Technologies*, *26*, 874–879.

Liu, X., Qian, L., Shu, T., & Tong, Z. (2003). Rheology characterization of sol–gel transition in aqueous alginate solutions induced by calcium cations through in situ release. *Polymer*, *44*, 407–412.

Mongondry, P., Tassin, J. F., & Nicolai, T. (2005). Revised state diagram of laponite dispersions. *Journal of Colloid and Interface Science*, *283*, 397–405.

Morariu, S., Bercea, M., & Sacarescu, L. (2014). Tailoring of clay/poly (ethylene oxide) hydrogel properties by chitosan incorporation. *Industrial & Engineering Chemistry Research*, *53*, 13690–13698.

Papajová, E., Bujdoš, M., Chorvát, D., Stach, M., & Lacík, I. (2012). Method for preparation of planar alginate hydrogels by external gelling using an aerosol of gelling solution. *Carbohydrate Polymers*, *90*, 472–482.

Payet, L., Ponton, A., Grossiord, J.-L., & Agnely, F. (2010). Structural and rheological properties of chitosan semi-interpenetrated networks. *The European Physical Journal E*, *32*, 109–118.

Percival, E. (1979). The polysaccharides of green, red and brown seaweeds: Their basic structure, biosynthesis and function. *British Phycological Journal*, *14*, 103–117.

Perkins, R., Brace, R., & Matijević, E. (1974). Colloid and surface properties of clay suspensions. I. Laponite CP. *Journal of Colloid and Interface Science*, *48*, 417–426.

Rezende, R. A., Bártolo, P. J., Mendes, A., & Maciel Filho, R. (2009). Rheological behavior of alginate solutions for biomanufacturing. *Journal of Applied Polymer Science*, *113*, 3866–3871.

Rodríguez-Rivero, C., Hilliou, L., del Valle, E. M. M., & Galán, M. A. (2014). Rheological characterization of commercial highly viscous alginate solutions in shear and extensional flows. *Rheologica Acta*, *53*, 559–570.

Roger, S., Sang, Y. Y. C., Bee, A., Perzynski, R., Di Meglio, J. M., & Ponton, A. (2015). Structural and multi-scale rheophysical investigation of diphasic magneto-sensitive materials based on biopolymers. *The European Physical Journal E*, *38*, 1–13.

Ruzicka, B., & Zaccarelli, E. (2011). A fresh look at the laponite phase diagram. *Soft Matter*, *7*, 1268–1286.

Shahin, A., & Joshi, Y. M. (2010). Irreversible aging dynamics and generic phase behavior of aqueous suspensions of laponite. *Langmuir*, *26*, 4219–4225.

Shen, M., Li, L., Sun, Y., Xu, J., Guo, X., & Prud'homme, R. K. (2014). Rheology and adhesion of poly (acrylic acid)/laponite nanocomposite hydrogels as biocompatible adhesives. *Langmuir*, *30*, 1636–1642.

Sun, W., Wang, T., Wang, C., Liu, X., & Tong, Z. (2013). Scaling of the dynamic response of hectorite clay suspensions containing poly (ethylene glycol) along the universal route of aging. *Soft Matter*, *9*, 6263–6269.

Sun, W., Yang, Y., Wang, T., Huang, H., Liu, X., & Tong, Z. (2012). Effect of adsorbed poly (ethylene glycol) on the gelation evolution of laponite suspensions: Aging time-polymer concentration superposition. *Journal of Colloid and Interface Science*, *376*, 76–82.

Tawari, S. L., Koch, D. L., & Cohen, C. (2001). Electrical double-layer effects on the Brownian diffusivity and aggregation rate of laponite clay particles. *Journal of Colloid and Interface Science*, *240*, 54–66.

Thompson, D. W., & Butterworth, J. T. (1992). The nature of laponite and its aqueous dispersions. *Journal of Colloid and Interface Science*, *151*, 236–243.

Thu, B., Bruheim, P., Espevik, T., Smidsrød, O., Soon-Shiong, P., & Skjåk-Bræk, G. (1996). Alginate polycation microcapsules: I. Interaction between alginate and polycation. *Biomaterials*, *17*, 1031–1040.

Venkatesan, J., Bhatnagar, I., Manivasagan, P., Kang, K.-H., & Kim, S.-K. (2015). Alginate composites for bone tissue engineering: A review. *International Journal of Biological Macromolecules*, *72*, 269–281.

Willenbacher, N. (1996). Unusual thixotropic properties of aqueous dispersions of laponite RD. *Journal of Colloid and Interface Science*, *182*, 501–510.

Winter, H. H., & Chambon, F. (1986). Analysis of linear viscoelasticity of a crosslinking polymer at the gel point. *Journal of Rheology (1978-present)*, *30*, 367–382.

Xavier, J. R., Thakur, T., Desai, P., Jaiswal, M. K., Sears, N., Cosgriff-Hernandez, E., Kaunas, R., & Gaharwar, A. K. (2015). Bioactive nanoengineered hydrogels for bone tissue engineering: A growth-factor-free approach. *ACS Nano*, *9*, 3109–3118.

Yu, F., Zhang, F., Luan, T., Zhang, Z., & Zhang, H. (2014). Rheological studies of hyaluronan solutions based on the scaling law and constitutive models. *Polymer*, *55*, 295–301.

Zulian, L., Ruzicka, B., & Ruocco, G. (2008). Influence of an adsorbing polymer on the aging dynamics of laponite clay suspensions. *Philosophical Magazine*, *88*, 4213–4221.